$WCH_aH_xC(CH_3)_3$, $^2J_{H_aH_x} = 15$ Hz), 1.74 (s, 2 H, $WCH_2C(CH_3)_3$), 1.04 (s, 9 H, $WCH_2C(CH_3)_3$), 0.86 (s, 18 H, $WCH_aH_bC(CH_3)_3$), 0.67 (d, 2 H, $WCH_aH_xC(CH_3)_3$), overlapped by the previous Bu^t group ($(N(CH_2CH_2)_{\text{anti and syn}}$). IR (Nujol) ($\nu$ cm^{-1}): 1230 (m, W–CH_2Bu^t), 960 (s, WO).

X-ray Structure Determination. Suitable orange yellow crystals of **2a** were obtained by slow evaporation of a saturated pentane solution of **2a** and were mounted above a stream of argon. Data were collected on a Philips PW1100/16 diffractometer equipped with a low-temperature device using nickel-filtered Cu Kα radiation ($\lambda = 1.5418$ Å). The crystal data and data collection parameters are summarized in Table IV. No significant changes were observed for three standard reflections monitored hourly during the data collection period. The Enraf-Nonius SDP package[21] was used on a Microvax II computer for all calculations, except that a local program was employed for data reduction. The initial step–scan data were converted to intensities by the method of Lehmann and Larson[22] and then corrected for Lorentz polarization and absorption factors, with the latter being computed by the method of Walker and Stuart.[23] The structure was solved using the heavy atom method. The remaining non-hydrogen atoms were located on subsequent difference Fourier maps. Hydrogen atoms were introduced at computed coordinates (C–H = 0.95 Å) with isotropic temperature factors $B(H) = 1 + B_{eqv}(C)$ Å^2. Full least-squares refinements converged to the R factors, shown in Table IV. Final difference maps revealed no significant maxima.

Acknowledgment. We thank the CNRS for financial support.

Registry No. **1a**, 141583-60-0; **1b**, 141583-61-1; **2a**, 141583-62-2; **2a**·$AlCl_3$, 141583-58-6; **2b**, 141583-63-3; **2c**, 141583-64-4; **2c**·$AlCl_3$, 141583-59-7; $Mg(CH_2Bu^t)_2$·(dioxane), 67608-37-1; $ClCH_2Bu^t$, 753-89-9.

Supplementary Material Available: Listings of positional and thermal equivalent parameters for all non-hydrogen atoms (Table S1), temperature factors for anisotropic atoms (Table S2), hydrogen atom positional parameters (Table S3), and bond distances and angles (Table S4) for **2a** (6 pages). Ordering information is given on any current masthead page.

OM9106138

---

(21) Frentz, B. A. In *Computing in Crystallography*; Schenk, H., Olthof-Hazekamp, R., van Koningaveld, H., Bassi, C. G., Eds.; Delft University Press: Delft, The Netherlands, 1978; p 64.

(22) Lehmann, M. S.; Larsen, F. K. *Acta Crystallogr.* 1974, *A30*, 580.

(23) Walker, N.; Stuart, D. *Acta Crystallogr.* 1983, *A39*, 158.

Kinetics and Mechanism of Substitution Reactions of the 17-Electron Complexes $\{\eta^5\text{-}C_5R_5Cr(CO)_3\}$ (R = H, Me) with Tertiary Phosphines

W. Carl Watkins, Kristine Hensel, Suzanne Fortier,* Donal H. Macartney,* and
Michael C. Baird*

Department of Chemistry, Queen's University, Kingston, Ontario, Canada K7L 3N6

Stephan J. McLain

*Central Research and Development Department, Experimental Station,
E. I. du Pont de Nemours & Company, Wilmington, Delaware 19898*

Received December 20, 1991

A kinetics investigation of the substitution reactions of the compounds $\{\eta^5\text{-}C_5R_5Cr(CO)_3\}$ (R = H, Me) with tertiary phosphines L to form the substituted radicals $\{\eta^5\text{-}C_5R_5Cr(CO)_2L\}$ is described. The nature of the observed rate laws, the activation parameters, and the steric effects suggest that an associative mechanism pertains, although an interchange–associative process may apply in the case of the back-reaction of the bulky $\{\eta^5\text{-}C_5Me_5Cr(CO)_2(PMe_2Ph)\}$ with CO. The substitution reactions are accompanied by disproportionation processes to form $[\eta^5\text{-}C_5H_5Cr(CO)_2L_2][\eta^5\text{-}C_5H_5Cr(CO)_3]$ (via the monosubstituted cationic complexes $[\eta^5\text{-}C_5H_5Cr(CO)_3L][\eta^5\text{-}C_5H_5Cr(CO)_3]$) and/or by formation of the substituted hydrides $\eta^5\text{-}C_5R_5Cr(CO)_2LH$, depending on the reaction conditions. The X-ray crystal structure of the substituted hydride $\eta^5\text{-}C_5R_5Cr(CO)_2(CDPP)H$ (CDPP = cyclohexyldiphenylphosphine) is described; the compound assumes a cisoid geometry.

Organotransition-metal chemistry has long been dominated by compounds containing closed-shell configurations and obeying the 18-electron rule,[1] but recent years have seen the development of a very extensive chemistry of 17-electron complexes.[2] The latter class of paramagnetic, metal-centered radicals is now known to play important roles as reactive intermediates in many types of reactions, but several examples have proven sufficiently persistent that they have been isolated and characterized both spectroscopically and crystallographically.[2] Of particular relevance here, and in contrast to the chemistry of most 18-electron complexes,[1] which generally undergo ligand substitution reactions via dissociative pathways,[3] several 17-electron compounds have been found to undergo substitution reactions that proceed via associative processes.[4]

---

(1) Collman, J. P.; Hegedus, L. S.; Norton, J. R.; Finke, R. G. *Principles and Applications of Organotransition Metal Chemistry*; University Science Books: Mill Valley, California, 1987.

(2) (a) Baird, M. C. *Chem. Rev.* 1988, *88*, 1217. (b) Trogler, W. C., Ed. *Organometallic Radical Process*; Elsevier: Amsterdam, 1990.

(3) (a) See: ref 1, chapter 4. (b) Howell, J. A. S.; Burkinshaw, P. M. *Chem. Rev.* 1983, *83*, 557.

(4) (a) Trogler, W. C. In *Organometallic Radical Process*; Trogler, W. C., Ed.; Elsevier: Amsterdam, 1990; p 306 and references therein. (b) Tyler, D. R. In *Organometallic Radical Process*; Trogler, W. C., Ed.; Elsevier: Amsterdam, 1990; p 338 and references therein. (c) Stiegman, A. E.; Tyler, D. R. *Comments Inorg. Chem.* 1986, *5*, 215. (d) Shi, Q.-Z.; Richmond, T. G.; Trogler, W. C.; Basolo, F. *J. Am. Chem. Soc.* 1984, *106*, 71.

0276-7333/92/2311-2418$03.00/0

The lone pair of the incoming ligand is believed to interact with the singly occupied orbital of the electronically unsaturated substrate in a 19-electron intermediate or transition state.[4] However, relatively few relevant studies have as yet been reported, and the generality of the associative mechanism has not yet been firmly established.

We[5] and others[6] have reported extensively on the series of persistent, 17-electron chromium-centered radicals $\{\eta^5\text{-}C_5R_5Cr(CO)_2L\}$ (R = H, Me; L = CO, tertiary phosphine); when L = CO, the radicals exist in solution in equilibrium with the corresponding diamagnetic, closed-shell dimers, $[\eta^5\text{-}C_5R_5Cr(CO)_3]_2$ (eq 1). Since the mono-

$$[\eta^5\text{-}C_5R_5Cr(CO)_3]_2 \overset{K}{\rightleftharpoons} 2\{\eta^5\text{-}C_5R_5Cr(CO)_3\} \qquad (1)$$

mer–dimer exchange processes are rapid on the NMR time scale at ambient temperatures, much of the chemistry of both systems (R = H and Me) has been shown to reflect the reactivity of the significantly more labile monomers.[5a,d,f,g,j] The two systems thus appeared to provide further opportunities to investigate the mechanisms of ligand substitution reactions of 17-electron compounds, and we report herein a kinetics study of the substitution reactions (eq 2); a preliminary report has appeared previously.[5h] During the course of this work, further results

$$\{\eta^5\text{-}C_5R_5Cr(CO)_3\} + L \underset{k_{-2}}{\overset{k_2}{\rightleftharpoons}} \{\eta^5\text{-}C_5R_5Cr(CO)_2L\} + CO \qquad (2)$$

on disproportionation reactions[5] (eq 3) of $[\eta^5\text{-}C_5H_5Cr(CO)_3]_2$ were also obtained and are discussed.

$$[\eta^5\text{-}C_5H_5Cr(CO)_3]_2 + 2L \rightarrow [\eta^5\text{-}C_5H_5Cr(CO)_2L_2]^+ + [\eta^5\text{-}C_5H_5Cr(CO)_3]^- + CO \qquad (3)$$

Experimental Section

Syntheses were carried out utilizing normal Schlenk techniques and dried, deaerated solvents. IR and NMR spectra were run on Bruker IFS-85 FT-IR and either HX-60 or AM-400 FT-NMR spectrometers, respectively. Variable-temperature IR spectra were obtained by utilizing a Fenwall Model 550 variable-temperature IR cell or a Specac Model P/N 21.500 variable-temperature unit connected to a Specac P/N 20.120 series Eurotherm automatic temperature controller. Stopped-flow kinetics were performed on a homemade stopped-flow apparatus and a Hewlett-Packard 8452A diode array UV–vis spectrophotometer.

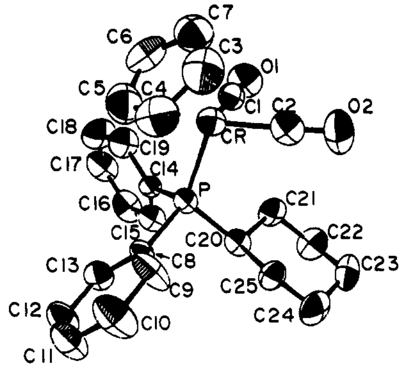

Figure 1. ORTEP diagram of $\eta^5\text{-}C_5H_5Cr(CO)_2(CDPP)H$.

The compounds $[\eta^5\text{-}C_5H_5Cr(CO)_3]_2$ and $[\eta^5\text{-}C_5Me_5Cr(CO)_3]_2$ were prepared as in the literature.[5f,l] Most tertiary phosphines were purchased from Strem Chemicals; cyclohexyldiphenylphosphine (CDPP) and dicyclohexylphenylphosphine (DCPP) were gifts from M & T Chemicals.

Kinetics Experiments. All kinetics experiments involving reactions of $[\eta^5\text{-}C_5H_5Cr(CO)_3]_2$ with CDPP and PPh_3 were performed in N_2-saturated toluene solutions under a nitrogen atmosphere and under pseudo-first-order conditions. The dimer concentrations were approximately 0.0035 M, while the phosphine concentrations ranged from 0.01 to 0.15 M. In a typical experiment, $[\eta^5\text{-}C_5H_5Cr(CO)_3]_2$ was weighed into a 100-mL round-bottom flask, toluene was then added, and the solution was stirred for at least 20 min at the desired temperature in order to ensure that all the dimer had dissolved. To this was added an appropriate volume of a toluene solution of the phosphine at the same temperature such that the concentrations of both species were in the ranges outlined above. The reactions were then monitored by IR spectroscopy, samples of the reaction mixtures being extracted utilizing gastight syringes and the absorbance values for the bands at ν(CO) at 1946 cm^{-1} (dimer) and ≈1800 cm^{-1} (product) being recorded.

The reactions of $[\eta^5\text{-}C_5H_5Cr(CO)_3]_2$ with $PMePh_2$ and of $[\eta^5\text{-}C_5Me_5Cr(CO)_3]_2$ with PMe_2Ph and $PMePh_2$ were too rapid to be studied by the above procedure and were therefore monitored by using stopped-flow visible spectroscopy in N_2- or CO-saturated solutions. With $[\eta^5\text{-}C_5H_5Cr(CO)_3]_2$ (≈0.000 16 M; phosphine concentration 0.006–0.016 M in N_2-saturated toluene), the disappearance of the dimer was monitored at 456 nm, the apparent isosbestic point for the two dimer rotamers.[5d] With $[\eta^5\text{-}C_5Me_5Cr(CO)_3]_2$ (≈0.0017 M, phosphine 0.01–0.12 M in CO-saturated toluene), the disappearance of the monomer, $\{\eta^5\text{-}C_5Me_5Cr(CO)_3\}$, was monitored at three wavelengths, 580, 600, and 610 nm. At least four replicate runs were taken for each phosphine concentration at each temperature. With both systems, a UV filter with a cutoff at 300 nm was utilized in order to minimize photochemical side reactions.

Preparation and Crystal Structure of $\eta^5\text{-}C_5H_5Cr(CO)_2(CDPP)H$. A solution of 0.28 g (0.70 mmol) of $[\eta^5\text{-}C_5H_5Cr(CO)_3]_2$ and 0.52 g (1.9 mmol) of CDPP was refluxed for 1 h in 60 mL of ethanol. At this point, an IR spectrum exhibited ν(CO) at 1916 and 1799 cm^{-1}, which may be attributed to the substituted radical $\{\eta^5\text{-}C_5H_5Cr(CO)_2(CDPP)\}$,[5] as well as ν(CO) at 1932 and 1862 cm^{-1}, which may be attributed to $\eta^5\text{-}C_5H_5Cr(CO)_2(CDPP)H$ (see below). The ethanol was removed under reduced pressure, the resulting residue was extracted with toluene and then recrystallized from 1:2 ethyl ether–hexane to give pale green crystals of the product. IR (toluene): ν(CO) 1925, 1858 cm^{-1}. ^1H NMR (toluene-d_8): δ −5.56 (d, J_{PH} = 80 Hz, CrH), δ 0.87 (m, 1 H), δ 1.09 (m, 4 H), 1.45 (d, J = 13 Hz, 1 H), δ 1.60 (d, J = 11 Hz, 2 H), δ 1.96 (d, J = 7.2 Hz, 2 H), δ 2.2 (q, J = 10 Hz, 2 H), δ 4.18 (s, 5 H, C_5H_5), δ 7.0–7.5 (m, 10 H, Ph).

The compound crystallizes in space group $P\bar{1}$ with a = 10.962 (5) Å, b = 11.454 (6) Å, c = 9.553 (5) Å, α = 105.71 (4)°, β = 106.21

---

(5) (a) Cooley, N. A.; Watson, K. A.; Fortier, S.; Baird, M. C. *Organometallics*, **1986**, *5*, 2563. (b) Morton, J. R.; Preston, K. F.; Cooley, N. A.; Baird, M. C.; Krusic, P. J.; McLain, S. J. *J. Chem. Soc., Faraday Trans. I* **1987**, *83*, 3535. (c) Krusic, P. J.; McLain, S. J.; Morton, J. R.; Preston, K. F. *J. Magn. Reson.* **1987**, *74*, 72. (d) McLain, S. J. *J. Am. Chem. Soc.* **1988**, *110*, 643. Figure 1 of this communication is mislabeled; the correct concentration on a chromium atom basis is 0.001 03 M. We also thank V. M. Miskowski for pointing out that the temperature-dependent behavior of the $\sigma \rightarrow \sigma^*$ band, which was originally described as isosbestic behavior and attributed to rotational isomers, is probably a result of thermal population of Cr–Cr excited vibrational levels (see: Miskowski, V. M.; Smith, T. P.; Loehr, T. M.; Gray, H. B. *J. Am. Chem. Soc.* **1985**, *107*, 7925. (e) Cooley, N. A.; Baird, M. C.; Morton, J. R.; Preston, K. F.; LePage, Y. *J. Magn. Reson.* **1988**, *76*, 325. (f) Cooley, N. A.; MacConnachie, P. F. T.; Baird, M. C. *Polyhedron* **1988**, *7*, 1965. (g) Jaeger, T. J.; Baird, M. C. *Organometallics* **1988**, *7*, 204. (h) Watkins, W. C.; Macartney, D. H.; Baird, M. C. *J. Organomet. Chem.* **1989**, *377*, C52. (i) Jaeger, T. J.; Watkins, W. C.; MacNeil, J. H.; Fortier, S.; Watson, K. A.; Hensel, K.; Baird, M. C.; Preston, K. F.; Morton, J. R.; LePage, Y.; Charland, J.-P. *J. Am. Chem. Soc.* **1991**, *113*, 542. (j) Goulin, C. A.; Huber, T. A.; Nelson, S. M.; Macartney, D. H.; Baird, M. C. *J. Chem. Soc., Chem. Commun.* **1991**, 798. (k) O'Callaghan, K.; Brown, S. J.; Page, J. A.; Baird, M. C.; Richards, T. C.; Geiger, W. E. *Organometallics* **1991**, *10*, 3114. (l) Watkins, W. C.; Jaeger, T. J.; Kidd, C. E.; Fortier, S.; Baird, M. C.; Kiss, G.; Roper, G. C.; Hoff, C. D. *J. Am. Chem. Soc.* **1992**, *114*, 907.

(6) (a) Madach, T.; Vahrenkamp, H. Z. *Naturforsch.* **1978**, *33b*, 1301. (b) Madach, T.; Vahrenkamp, H. Z. *Naturforsch.* **1979**, *34b*, 573. (c) Goh, L. Y.; D'Aniello, M. J.; Slater, S.; Muetterties, E. L.; Tavanaiepour, I.; Chang, M. I.; Fredrich, M. F.; Day, V. W. *Inorg. Chem.* **1979**, *18*, 192. (d) Goh, L. Y.; Hambley, T. W.; Darensbourg, D. J.; Reibenspies, J. *J. Organomet. Chem.* **1990**, *381*, 349. (e) Goh, L. Y.; Khoo, S. K.; Lim, Y. Y. *J. Organomet. Chem.* **1990**, *399*, 115. (f) Kiss, G.; Zhang, K.; Mukerjee, S. L.; Hoff, C. D.; *J. Am. Chem. Soc.* **1990**, *112*, 5657. (g) Goh, L. Y.; Lim, Y. Y. *J. Organomet. Chem.* **1991**, *402*, 209. (h) Schubert, U.; Ackermann, K.; Janta, R.; Voran, S.; Malisch, W. *Chem. Ber.* **1982**, *115*, 2003. (i) Eisenberg, D. C.; Lawrie, C. J. C.; Moody, A. E.; Norton, J. R. *J. Am. Chem. Soc.* **1991**, *113*, 4888.

Table I. Positional Parametes and Their Estimated Standard Deviations[a]

atom	x	y	z	B, Å^2
Cr	0.3632 (1)	0.34123 (9)	0.2306 (1)	3.62 (3)
P	0.2192 (2)	0.2017 (1)	0.1259 (2)	2.90 (4)
O1	0.3607 (5)	0.3115 (4)	0.5301 (4)	5.8 (1)
O2	0.2087 (5)	0.5836 (4)	0.3286 (5)	6.3 (1)
C1	0.3608 (6)	0.3193 (5)	0.4129 (7)	3.8 (2)
C2	0.2684 (6)	0.4880 (6)	0.2897 (6)	4.4 (2)
C3	0.4913 (7)	0.4348 (6)	0.1774 (9)	6.6 (2)
C4	0.4620 (7)	0.3378 (7)	0.0562 (8)	6.3 (2)
C5	0.5072 (7)	0.2301 (7)	0.1075 (9)	6.4 (2)
C6	0.5659 (7)	0.2608 (7)	0.2570 (8)	6.4 (2)
C7	0.5555 (7)	0.3871 (7)	0.3008 (8)	6.3 (2)
C8	0.1947 (5)	0.1443 (5)	−0.0768 (6)	2.7 (1)
C9	0.1832 (7)	0.2252 (5)	−0.1661 (6)	5.1 (2)
C10	0.1626 (8)	0.1885 (6)	−0.3180 (7)	6.3 (2)
C11	0.1524 (8)	0.0691 (6)	−0.3883 (7)	5.7 (2)
C12	0.1636 (7)	−0.0151 (6)	−0.3039 (7)	4.8 (2)
C13	0.1865 (6)	0.0238 (6)	−0.1484 (6)	4.1 (2)
C14	0.2611 (5)	0.0574 (5)	0.1943 (6)	2.9 (1)
C15	0.1688 (6)	−0.0096 (5)	0.1886 (7)	4.0 (2)
C16	0.2054 (7)	−0.1200 (6)	0.2402 (7)	5.2 (2)
C17	0.3325 (8)	−0.1584 (6)	0.2970 (7)	5.9 (2)
C18	0.4243 (7)	−0.0919 (6)	0.3030 (8)	6.2 (2)
C19	0.3869 (7)	0.0175 (5)	0.2531 (7)	4.8 (2)
C20	0.0541 (6)	0.2591 (5)	0.1474 (6)	3.1 (1)
C21	0.0454 (6)	0.3005 (5)	0.3099 (6)	4.1 (2)
C22	−0.0905 (6)	0.3477 (6)	0.3297 (7)	5.1 (2)
C23	−0.1541 (7)	0.4511 (6)	0.2471 (8)	5.2 (2)
C24	−0.1528 (7)	0.4045 (6)	0.0857 (8)	5.4 (2)
C25	−0.0177 (6)	0.3620 (5)	0.0639 (7)	4.1 (2)

[a] Anisotropically refined atoms are given in the form of the isotropic equivalent thermal parameter defined as (4/3)[$a2B(1,1) + b2B(2,2) + c2B(3,3) + ab(\cos\gamma) \times B(1,2) + ac(\cos\beta) \times B(1,3) + bc(\cos\alpha) \times B(2,3)$].

Table II. Bond Distances (Å) and Angles (deg) for η^5-$C_5H_5Cr(CO)_2(CDPP)H$

	Bond Lengths[a,b]		
Cr–C1	1.834 (6)	C14–C19	1.360 (6)
Cr–C2	1.805 (6)	C3–C4	1.390 (8)
Cr–C3	2.178 (5)	C3–C7	1.378 (8)
Cr–C4	2.214 (5)	C4–C5	1.389 (8)
Cr–C5	2.196 (6)	C5–C6	1.375 (8)
Cr–C6	2.178 (5)	C6–C7	1.380 (8)
Cr–C7	2.164 (6)	C8–C9	1.385 (6)
Cr–P	2.330 (1)	C8–C13	1.375 (6)
P–C8	1.831 (4)	C9–C10	1.365 (7)
P–C14	1.857 (4)	C10–C11	1.365 (7)
P–C20	1.830 (5)	C11–C12	1.381 (7)
O1–C1	1.147 (5)	C12–C13	1.397 (6)
O2–C2	1.167 (5)	C20–C21	1.519 (6)
C14–C15	1.382 (6)	C21–C22	1.513 (7)
C15–C16	1.416 (7)	C23–C24	1.492 (7)
C16–C17	1.364 (8)	C20–C25	1.546 (6)
C17–C18	1.372 (8)	C22–C23	1.531 (7)
C18–C19	1.396 (7)	C24–C25	1.506 (7)
	Bond Angles		
P–Cr–C1	86.7 (2)	C10–C11–C12	119.3 (5)
P–Cr–C2	106.2 (2)	C11–C12–C13	119.2 (5)
C1–Cr–C2	83.2 (2)	C8–C13–C12	122.0 (4)
Cr–P–C8	114.9 (1)	P–C14–C15	122.2 (3)
Cr–P–C14	116.5 (2)	P–C14–C19	118.6 (4)
Cr–P–C20	116.0 (1)	C15–C14–C19	119.2 (4)
C8–P–C14	102.3 (2)	C14–C15–C16	120.2 (5)
C8–P–C20	102.0 (2)	C15–C16–C17	119.1 (5)
C14–P–C20	103.1 (2)	C16–C17–C18	120.7 (5)
C4–C3–C7	108.4 (6)	C17–C18–C19	119.6 (5)
C3–C4–C5	107.3 (6)	C14–C19–C18	121.1 (5)
C4–C5–C6	108.0 (6)	P–C20–C21	112.9 (3)
C5–C6–C7	108.6 (6)	P–C20–C25	114.3 (3)
C3–C7–C6	107.7 (6)	C21–C20–C25	109.5 (4)
P–C8–C9	119.3 (3)	C20–C21–C22	113.7 (4)
P–C8–C13	124.0 (3)	C21–C22–C23	110.6 (4)
C9–C8–C13	116.7 (4)	C22–C23–C24	109.0 (4)
C8–C9–C10	122.1 (4)	C23–C24–C25	111.6 (4)
C9–C10–C11	120.7 (5)	C20–C25–C24	111.5 (4)

[a] Numbers in parentheses are estimated standard deviations in the least significant digits. [b] Shortest Cr–Cr distance = 5.9 Å.

(4)°, $\gamma = 77.10$ (4)°; $V = 1094.5$ Å^3; $Z = 2$, D(calc) = 1.336 Mg m^{-3}, $\mu = 5.98$ cm. A green crystal, 0.50 mm × 0.35 mm × 0.13 mm, was mounted inside a glass capillary and used for the collection of intensity data on an Enraf-Nonius CAD-4 diffractometer. The unit cell parameters were obtained by a least-squares analysis of 25 centered reflections in the range $15.60 < 2\theta < 26.80°$. The data were collected by the θ–2θ scan technique, with variable scanning rate, using monochromatic Mo Kα radiation. A total of 2180 unique reflections were measured in the range $1.0 \leq 2\theta \leq 40°$, of which 1437 were considered observed, i.e., $I \geq 3\sigma_I$. Three standard reflections were measured every 7200 s of radiation time and showed no significant variation during the course of data collection. The intensities were corrected for Lorentz and polarization effects but not for absorption.

The structure was solved by direct methods using the program MULTAN80.[7] Difference Fourier map calculations revealed the positions of all the hydrogen atoms except for the hydride ligand atom. These were assigned temperature factors equal in magnitude to the equivalent isotropic values of their parent atoms and were included in the calculations but not refined. Full-matrix least-squares refinement minimizing the function $\sum w||F_o| - |F_c||^2$, where $w = 1/\sigma^2(|F_o|)$, resulted in $R = 0.046$ and $R_w = 0.056$. The esd of an observation of unit weight was 2.110, the maximum shift to error ratio was 0.02, and the final difference Fourier synthesis was essentially featureless. The scattering factors used were those of Cromer and Waber,[8] while the anomalous dispersion coefficients were taken from Cromer.[9] All calculations were carried out on a PDP 11/23 computer using the structure determination package of Enraf-Nonius, SDP.[10] The program ORTEP[11] was used for the preparation of the illustration. The final atomic coordinates of the heavy atoms are given in Table I, bond distances and angles in Table II. An ORTEP structure is shown in Figure 1.

Preparation of [η^5-$C_5H_5Cr(CO)_2(PMePh_2)_2$][$\eta^5$-$C_5H_5Cr(CO)_3$]. $PMePh_2$ (0.125 g, 0.62 mmol) was added dropwise to a suspension of [η^5-$C_5H_5Cr(CO)_3]_2$ in pentane. The reaction mixture was stirred for 12 h, and the yellow solid product was isolated in quantitative yield by filtration followed by vacuum drying. Calcd for $C_{41}H_{36}Cr_2O_5P_2$: C, 63.57; H, 4.68; P, 8.00; Cr, 13.42. Observed: C, 62.73; H, 4.73; P, 7.72; Cr, 13.2.

Results and Discussion

Preliminary Experiments. A series of experiments was carried out initially to determine the optimum temperatures and concentrations for the kinetics runs; tertiary phosphines of widely varying cone angles[12] were assessed in this way in order to test the anticipated[2] dependence of rates on ligand steric requirements.

As expected on the basis of earlier work,[5f] reactions of the very small PMe_3 (cone angle 118°)[12] with millimolar concentrations of [η^5-$C_5H_5Cr(CO)_3]_2$ in toluene proceeded very rapidly at ambient temperature to produce the rather labile {η^5-$C_5H_5Cr(CO)_2(PMe_3)$}, identified by ν_{CO} at 1914

---

(7) Main, P.; Fiske, S. J.; Hull, S. E.; Lessinger, S. L.; Germain, G.; Declercq, J. P.; Woolson, M. M. MULTAN80. A System of Computer Programs for the Automatic Solution of Crystal Structures from X-ray Diffraction Data. Universities of York, England, and Louvain, Belgium, 1980.

(8) Cromer, D. T.; Waber, J. T. *International Table for X-ray Crystallography*; Kynoch Press: Birmingham, 1974; Vol. IV (present distributor D. Reidel, Dordrecht).

(9) Cromer, D. T. *International Table for X-ray Crystallography*; Kynoch Press: Birmingham, 1974; Vol. IV (present distributor D. Reidel, Dordrecht).

(10) Frenz, B. A. Enraf-Nonius Structure Determination Package Enraf-Nonius, Delft, 1979.

(11) Johnson, C. K. ORTEP. Report ORNL-3794. Oak Ridge National Laboratory, Oak Ridge, TN, 1965.

(12) (a) Tolman, C. A. *Chem. Rev.* **1977**, *77*, 313. (b) Reference 1, p 70.

cm^{-1} (s) and 1791 cm^{-1} (s, br). Interestingly, however, higher concentrations of $[\eta^5\text{-}C_5H_5Cr(CO)_3]_2$ also resulted in the rapid formation of a yellow crystalline precipitate, which exhibited ν_{CO} in its IR spectrum in THF at 1953 cm^{-1} (m), 1892 cm^{-1} (s), 1875 cm^{-1} (s), 1781 cm^{-1} (s), and 1763 cm^{-1} (m). Although this material was not investigated further, its IR spectrum is very similar to that reported elsewhere for $[\eta^5\text{-}C_5H_5Cr(CO)_2(PMe_3)_2][\eta^5\text{-}C_5H_5Cr(CO)_3]$ (1956 (s) and 1879 (vs) for the cation, 1897 (s), 1778 (s), and 1765 (s) cm^{-1} for the anion),[6h] the anticipated product of disproportionation,[5f] and that of $[\eta^5\text{-}C_5H_5Cr(CO)_2(PMePh_2)_2][\eta^5\text{-}C_5H_5Cr(CO)_3]$ (see below). It thus became clear that conditions for carrying out a kinetics investigation of substitution reactions of $[\eta^5\text{-}C_5H_5Cr(CO)_3]_2$ would have to be chosen with care.

Indeed, disproportionation products could be readily obtained with PMe_2Ph (cone angle 122°)[12] and $PMePh_2$ (cone angle 136°)[12] if concentrations of reactants in toluene were sufficiently high that the products of disproportionation would precipitate, and, indeed, $[\eta^5\text{-}C_5H_5Cr(CO)_2(PMePh_2)_2][\eta^5\text{-}C_5H_5Cr(CO)_3]$ was found to precipitate analytically pure on treatment of $[\eta^5\text{-}C_5H_5Cr(CO)_3]_2$ with $PMePh_2$ in pentane. It was also found that warming of a solution of $[\eta^5\text{-}C_5H_5Cr(CO)_2(PMePh_2)_2][\eta^5\text{-}C_5H_5Cr(CO)_3]$ in toluene resulted in rapid conversion to $\{\eta^5\text{-}C_5H_5Cr(CO)_2(PMePh_2)\}$ (ν(CO) 1919 (vs), 1798 (vs, br) cm^{-1}).

Interestingly, disproportionation can be the primary process for the reaction of $[\eta^5\text{-}C_5H_5Cr(CO)_3]_2$ with $PMePh_2$ in polar solvents, although the relationship between disproportionation and substitution is complex. Thus reactions of relatively concentrated (0.08 M) or dilute (0.008 M) THF solutions of $[\eta^5\text{-}C_5H_5Cr(CO)_3]_2$ with $PMePh_2$ give as the major product $[\eta^5\text{-}C_5H_5Cr(CO)_2(PMePh_2)_2][\eta^5\text{-}C_5H_5Cr(CO)_3]$ or $\{\eta^5\text{-}C_5H_5Cr(CO)_2(PMePh_2)\}$, respectively (IR). On treating a solution of $[\eta^5\text{-}C_5H_5Cr(CO)_3]_2$ (1.4×10^{-2} M in acetone-d_6) with a slight excess of $PMePh_2$ at 238 K, the resonance of the dimer at δ 5.20 disappeared almost immediately, being replaced by resonances at δ 7.6 (m, 10 H, Ph), δ 5.80 (d, J_{PH} = 1.3 Hz, 5 H, $\eta^5\text{-}C_5H_5$), δ 4.33 (s, 5 H, $\eta^5\text{-}C_5H_5$), and δ 2.67 (d, J_{PH} = 9.8 Hz, 3 H, Me), in addition to the resonances of free phosphine. The singlet at δ 4.33 may be assigned to the anion $[\eta^5\text{-}C_5H_5Cr(CO)_3]^-$,[5f] and thus the other resonances seem best attributed to the cationic species $[\eta^5\text{-}C_5H_5Cr(CO)_3(PMePh_2)]^+$. On warming to room temperature, the resonances of the cation weakened and were replaced by new resonances at δ 7.6 (m, 20 H, Ph), δ 5.17 (t, J_{PH} = 2.1 Hz, 5 H, $\eta^5\text{-}C_5H_5$), and δ 2.50 (deceptively simple triplet, 6 H, Me), which may be attributed to $[\eta^5\text{-}C_5H_5Cr(CO)_2(PMePh_2)_2][\eta^5\text{-}C_5H_5Cr(CO)_3]$. Monitoring of the IR spectrum of a complementary experiment resulted in assigning ν_{CO} at 2044 and 1935 cm^{-1} to $[\eta^5\text{-}C_5H_5Cr(CO)_3(PMePh_2)]^+$ and ν_{CO} at 1967 and 1893 cm^{-1} to the final cationic product, $[\eta^5\text{-}C_5H_5Cr(CO)_2(PMePh_2)_2]^+$.

In contrast to the above, the larger phosphines PPh_3 (cone angle 145°)[12] and CDPP (estimated cone angle 153°)[12] did not appear to take part in disproportionation processes but rather on occasion in relatively slow secondary reactions in which the radicals decomposed to the corresponding hydrides $\eta^5\text{-}C_5H_5Cr(CO)_2LH$. The reactions involving $PMePh_2$ in toluene also resulted in the slow formation of $\eta^5\text{-}C_5H_5Cr(CO)_2(PMePh_2)H$ in some instances. The hydrides were generally characterized spectroscopically, assignments being based on comparisons with data for $\eta^5\text{-}C_5H_5Cr(CO)_2(CDPP)H$, which was also characterized crystallographically (see below).

Kinetics of the Reactions of $\{\eta^5\text{-}C_5H_5Cr(CO)_3\}$ with CDPP, PPh_3, and $PMePh_2$. In toluene solutions at ambient temperature, millimolar concentrations of the 18-electron dimer, $[\eta^5\text{-}C_5H_5Cr(CO)_3]_2$, dissociate to an extent of a few percent (eq 1). The relevant thermodynamic parameters for the monomer–dimer equilibrium in this solvent are known,[5d] and hence toluene was the solvent of choice for the study of the reversible substitution reactions of eq 2. Unfortunately, it was found that derivation of an integrated rate equation describing the overall process of eqs 1 and 2 was only possible for the case where the reverse of the substitution step does not occur (see supplementary material), and kinetic runs involving the substitution reactions of $[\eta^5\text{-}C_5H_5Cr(CO)_3]_2$ with CDPP and PPh_3 were therefore carried out in a nitrogen atmosphere under conditions where it was possible to purge the system of carbon monoxide.

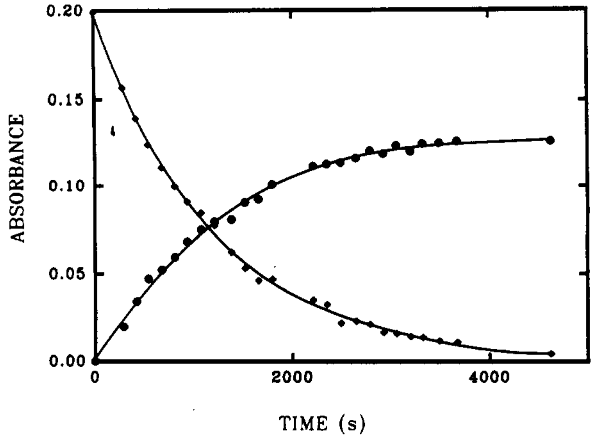

Figure 2. Plot of absorbance vs time for the reaction of $[\eta^5\text{-}C_5H_5Cr(CO)_3]_2$ with CDPP monitored at 1946 cm^{-1} (◆, disappearance of dimer) and 1796 cm^{-1} (●, appearance of product).

The integrated rate expression derived in the supplementary material provides a means of analyzing the rate data for the reactions of $[\eta^5\text{-}C_5H_5Cr(CO)_3]_2$ with the tertiary phosphines by taking into account the preequilibrium of eq 1. The rate equation thus obtained (eq 4) permits

$$\frac{[K^2 + 8K([\mathrm{Cr_{in}}] - [\mathrm{CrL}])]^{1/2} - K}{K} + \ln\,([K^2 + 8K([\mathrm{Cr_{in}}] - [\mathrm{CrL}])]^{1/2} - K) = -k_2[\mathrm{L}]t + \text{constant} \quad (4)$$

$$\text{constant} = \frac{[K^2 + 8K[\mathrm{Cr_{in}}]]^{1/2} - K}{K} + \ln\,((K + 8K[\mathrm{Cr_{in}}])^{1/2} - K)$$

the calculation of the observed rate constant k_2 assuming irreversibility, as is the case where the liberated CO is removed with a nitrogen purge.

In eq 4, K is the equilibrium constant for eq 1, $[\mathrm{Cr_{in}}]$ is the initial chromium concentration on a chromium atom basis, and [CrL] is the concentration of substituted radical. A plot of the left side of eq 4 vs time should therefore give a linear plot with slope = $-k_{obs}$, where $k_{obs} = k_2[\mathrm{L}]$. Values of [CrL] could be obtained either indirectly, utilizing the extinction coefficient of the dimer absorption at 1946 cm^{-1} (ϵ = 8500 ± 150 M^{-1} cm^{-1}), or directly, utilizing the extinction coefficients of the product absorptions at about 1800 cm^{-1} (ϵ = 2600 ± 380 M^{-1} cm^{-1} for $\{\eta^5\text{-}C_5H_5Cr(CO)_2(CDPP)\}$, 2820 ± 520 M^{-1} cm^{-1} for $\{\eta^5\text{-}C_5H_5Cr(CO)_2(PPh_3)\}$). The latter method, as might be anticipated, resulted in more consistent results and all data given below for CDPP and PPh_3 were determined in this way.

Typical plots of the smooth decay of the peak at 1946 cm^{-1} of the dimer, $[\eta^5\text{-}C_5H_5Cr(CO)_3]_2$, and of the concomitant appearance of the peak of $\{\eta^5\text{-}C_5H_5Cr(CO)_2(CDPP)\}$ at 1796 cm^{-1} are shown in Figure 2. In most cases, after

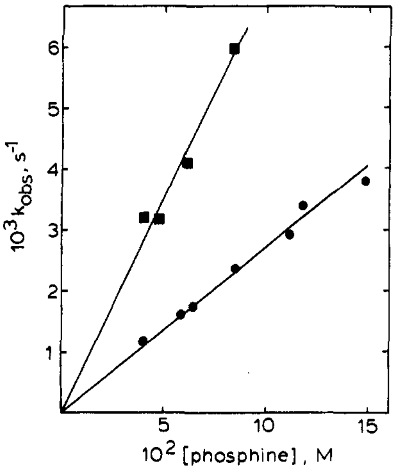

Figure 3. Plots of k_{obs} vs phosphine concentration for the reactions of $[\eta^5\text{-}C_5H_5Cr(CO)_3]_2$ with CDPP (●) and PPh_3 (■) at 308 K.

periods of time greater than two or three half-lives, the absorption of the product peak went through a maximum and then began to decay in turn. The products of the latter process in many cases included the hydride, $\eta^5\text{-}C_5H_5Cr(CO)_2(CDPP)H$, mentioned above and identified both spectroscopically (see Experimental Section) and crystallographically (see below), but the actual source of the hydridic hydrogen was not ascertained. Noncarbonyl-containing blue material was also deposited in many runs but also remained unidentified. These secondary products often formed during reactions of $[\eta^5\text{-}C_5H_5Cr(CO)_3]_2$ with CDPP and the other phosphines, but always at rates much lower than the rates for substitution of the tricarbonyl radical. On the other hand, disproportionation processes, as in eq 3, were never observed under the conditions of the kinetics experiments.

Treatment of the data as described above yielded values of k_{obs} that, when plotted vs. [L], gave a linear relationship with intercepts of zero, within experimental uncertainty. We present in Figure 3 plots of k_{obs} against phosphine concentration for L = CDPP and PPh_3 at 308 K. The values of k_2 (eq 4) for the substitution reactions of $\{\eta^5\text{-}C_5H_5Cr(CO)_3\}$ with CDPP and PPh_3 were determined at various temperatures in the range 303–318 K and are presented in Table III. The corresponding activation parameters, $\Delta H_2^‡$ and $\Delta S_2^‡$, are presented in Table IV.

Complementing the kinetics experiment with CDPP, measurements of the equilibrium constants for the substitution reaction of eq 2 (L = CDPP) were also made at the same temperatures. The experiments involved adding varying concentrations of CDPP in CO-saturated toluene to solutions of the dimer, also of known concentrations in CO-saturated toluene. The systems were allowed to proceed to thermal equilibrium, at which point the absorbances of the ν_{CO} at 1946 and 1796 cm^{-1} were measured. The solutions were then purged with N_2 (bubbling) in order to remove all traces of free CO and to drive the substitution reactions to completion. The absorbances of the peak at 1796 cm^{-1} were then measured, and CO was reintroduced to reestablish equilibrium from the direction of the products. By use of the known[13] concentrations of CO, the equilibrium constants K_{sub} for eq 2 were found to be 0.523 ± 0.018, 0.501 ± 0.021, and 0.473 ± 0.037 at 318, 313, and 308 K, respectively. A plot of ln K_{sub} vs T^{-1} yielded ΔH and ΔS values of 8.2 ± 5.7 kJ mol^{-1} and 20.4 ± 18 J mol^{-1} K^{-1}, respectively, and, since $\Delta H = \Delta H_2^‡ - \Delta H_{-2}^‡$ and $\Delta S = \Delta S_2^‡ - \Delta S_{-2}^‡$, values of $\Delta H_{-2}^‡$ and $\Delta S_{-2}^‡$ may be calculated and are also given in Table IV. While the relatively large statistical uncertainties in these data are somewhat disconcerting, they are an inevitable result of the necessarily narrow temperature range over which the kinetics study could be carried out.

Table III. Second-Order Rate Constants for Substitution Reactions of $\{\eta^5\text{-}C_5R_5Cr(CO)_3\}$ (R = H, Me) with Tertiary Phosphines

compound	ligand	T, K	k_2, M^{-1} s^{-1}	k_{-2}, M^{-1} s^{-1}
$\{\eta^5\text{-}C_5H_5Cr(CO)_3\}$	CDPP	308	2.70 ± 0.21^a	5.7 ± 0.9^{a,b}
		313	3.40 ± 0.36^a	6.8 ± 1.0^{a,b}
		318	4.23 ± 0.40^a	8.1 ± 1.0^{a,b}
	PPh_3	303	6.03 ± 0.55^a	c
		308	7.02 ± 0.60^a	c
		313	9.09 ± 0.81^a	c
$\{\eta^5\text{-}C_5Me_5Cr(CO)_3\}$	PMe_2Ph	297.9	0.957 ± 0.004	1.61 ± 0.03
		302.0	1.02 ± 0.04	2.50 ± 0.25
		308.1	1.14 ± 0.04	4.43 ± 0.27
		313.7	1.26 ± 0.05	6.88 ± 0.40
	$PMePh_2$	302.0	0.11 ± 0.03	1.4 ± 0.3

^{a} × 10^2. ^{b} Determined from k_2/K_{sub}. ^{c} Not determined.

Attempts to study the kinetics of the reaction of $[\eta^5\text{-}C_5H_5Cr(CO)_3]_2$ with $PMePh_2$ as above and utilizing low-temperature NMR spectroscopy proved impossible because the reaction proceeded too quickly at temperatures that were convenient. The reaction was therefore studied utilizing stopped-flow procedures in the temperature range 290–300 K in a closed system, as described in the Experimental Section. Concentrations of $[\eta^5\text{-}C_5H_5Cr(CO)_3]_2$ were kept sufficiently low (10^{-4} M) that disproportionation would not be a factor but, unfortunately, the reverse reaction of eq 2 becomes competitive during the course of the reaction under these conditions and the data cannot be treated as above. The assumption was therefore made that the first few percent of the reaction was not affected by the reverse reaction because of the very low concentration of CO, and only the initial slopes of plots of eq 4 were utilized to calculate approximate values of k_2. These were of the order of 1.6–2.0 M^{-1} s^{-1}, but the precision was such that calculation of activation parameters was not warranted.

An approximate measurement of the equilibrium constant for the substitution reaction of eq 2 (L = $PMePh_2$) was also carried out. Solutions prepared for kinetics runs were allowed to proceed to equilibrium, at which point the absorbances of the ν_{CO} at 1946 and ≈1800 cm^{-1} were measured. Assuming that the concentrations of CO and $\{\eta^5\text{-}C_5H_5Cr(CO)_2(PMePh_2)\}$ are equal, the equilibrium constant K_{sub} for eq 2 was found to be 263 ± 90 at 302 K.

Kinetics of the Reactions of $\{\eta^5\text{-}C_5Me_5Cr(CO)_3\}$ with PMe_2Ph and $PMePh_2$. In contrast to $[\eta^5\text{-}C_5H_5Cr(CO)_3]_2$, $[\eta^5\text{-}C_5Me_5Cr(CO)_3]_2$ is essentially completely dissociated in toluene at the temperatures used[51] and, during reactions with $PMePh_2$ and PMe_2Ph, the disappearance of $\{\eta^5\text{-}C_5Me_5Cr(CO)_3\}$ and the appearance of $\{\eta^5\text{-}C_5Me_5Cr(CO)_2L\}$ were found to obey simple pseudo-first-order kinetics. The reactions were studied by using stopped-flow procedures on solutions in CO-saturated toluene, making possible investigation of the back reaction of eq 2. Under these conditions, the solubility of CO in toluene[13] is such that its concentration is much greater than the chromium concentration, and the small amount of CO produced during the reaction had no effect on the rates.

In none of the reactions of PMe_2Ph did the absorbances of the $\{\eta^5\text{-}C_5Me_5Cr(CO)_3\}$ reach zero, indicating that equilibrium situations were being achieved. The data were

---

[13] (a) Wilhelm, E.; Battino, R. *Chem. Rev.* **1973**, *73*, 1. (b) Field, L. R.; Wilhelm, E.; Battino, R. *J. Chem. Thermodyn.* **1974**, *6*, 237. (c) Laidler, K. J.; Meiser, J. H. In *Physical Chemistry*; Benjamin/Cummings: Menlo Park, CA, 1982; p 904.

Table IV. Equilibrium Constants and Activation Parameters for the Substitution Reactions of $\{\eta^5\text{-}C_5R_5Cr(CO)_3\}$ (R = H, Me) with Tertiary Phosphines

compound	ligand	$\Delta H_2^{\ddagger}$,[a]	$\Delta H_{-2}^{\ddagger}$,[a]	$\Delta S_2^{\ddagger}$,[b]	$\Delta S_{-2}^{\ddagger}$,[b]
$\{\eta^5\text{-}C_5H_5Cr(CO)_3\}$	CDPP[c]	34.0 ± 10.2	26 ± 16[e]	−165 ± 33	−185 ± 51[e]
	PPh_3[d]	29.9 ± 9.9	e	−170 ± 32	e
$\{\eta^5\text{-}C_5Me_5Cr(CO)_3\}$	PMe_2Ph[d]	11.2 ± 1.9	70 ± 4	−208 ± 6	−7 ± 13

[a] kJ mol^{-1}. [b] J mol^{-1} K^{-1}. [c] 308 K. [d] 302 K. [e] Not determined.

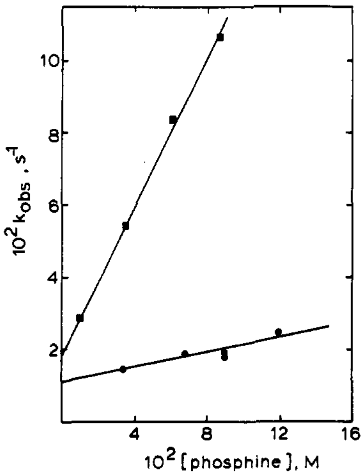

Figure 4. Plots of k_{obs} vs phosphine concentration for the reactions of $[\eta^5\text{-}C_5Me_5Cr(CO)_3]_2$ with $PMePh_2$ (●) and PMe_2Ph (■).

therefore analyzed by a linear least-squares fitting program to determine the infinity values, and plots of ln $(A_t - A_\infty)$ vs time were constructed. In all cases, these plots were linear for at least three half-lives, indicating first-order disappearance of $\{\eta^5\text{-}C_5Me_5Cr(CO)_3\}$, and plots of k_{obs} vs $[PMe_2Ph]$ were constructed (Figure 4) to obtain values of k_2 at the various temperatures, and hence the activation parameters. As can be seen from Figure 4, the plots exhibit nonzero intercepts, which give the k_{obs} for the reverse of eq 2. Utilizing the solubilities of CO in toluene at the temperatures used,[13] values of k_{-2} were also determined and hence the activation parameters for the reverse reaction. The rate constant data are presented in Table III, the corresponding activation parameters in Table IV.

Similar experiments were carried out for the reaction of $\{\eta^5\text{-}C_5Me_5Cr(CO)_3\}$ with $PMePh_2$ at 302 K, and the data were treated similarly. Calculated values of k_2 and k_{-2} are given in Table III; the ratio k_2/k_{-2} gives an equilibrium constant K_{sub} of 0.075 ± 0.036.

Comparisons of the Data. We have described above detailed kinetics experiments for the substitution reactions of $\{\eta^5\text{-}C_5H_5Cr(CO)_3\}$ with CDPP and PPh_3 and of $\{\eta^5\text{-}C_5Me_5Cr(CO)_3\}$ with PMe_2Ph and $PMePh_2$. We have also carried out a comparative but less definitive kinetics study of the reaction of $\{\eta^5\text{-}C_5H_5Cr(CO)_3\}$ with $PMePh_2$ and have noted qualitatively that the reaction of $\{\eta^5\text{-}C_5H_5Cr(CO)_3\}$ with PMe_3 is relatively rapid, while that with dicyclohexylphenylphosphine (DCPP, estimated cone angle 162°)[12] is extremely slow. Similarly the more sterically encumbered radical $\{\eta^5\text{-}C_5Me_5Cr(CO)_3\}$ is inert to substitution by more sterically demanding phosphines than $PMePh_2$, such as PPh_3.

In general, the rate laws for the four substitution processes studied in detail are consistent with an associative process, which would involve 19-electron transition states or intermediates. This interpretation is consistent with the relative rates, which decrease in the orders $PMe_3 > PMe_2Ph > PMePh_2 > PPh_3 >$ CDPP > DCPP and $\{\eta^5\text{-}C_5H_5Cr(CO)_3\} > \{\eta^5\text{-}C_5Me_5Cr(CO)_3\}$, since substitution reactions involving a bimolecular process are expected to be strongly affected by steric hindrance. Similar results have been reported for carbon monoxide substitution reactions of several other metal-centered radicals,[2,4] but we do not observe the dependence on phosphine basicity reported previously for the analogous substitution reactions of $V(CO)_6$.[4d] Possibly the relatively bulky $\eta^5\text{-}C_5H_5$ and $\eta^5\text{-}C_5Me_5$ groups result in steric factors being much more important in reactions of the chromium compounds than for reactions of $V(CO)_6$.

Consideration of the activation parameters for the forward and reverse reactions of eq 2 results in further confirmation of this interpretation, as the values obtained for the enthalpies of activation, $\Delta H_2^{\ddagger}$ and $\Delta H_{-2}^{\ddagger}$, vary significantly and are clearly not compatible with the type of dissociative process found for substitution reactions of many 18-electron carbonyl complexes.[3] The large, negative entropies of activation, $\Delta S_2^{\ddagger}$ and $\Delta S_{-2}^{\ddagger}$, found with only one exception, are also consistent with an associative process, and we note that similarly large, negative values of entropies of activation have been observed for associative substitution reactions of other metal-centered radicals.[4]

The exception in this study is the reaction of $\{\eta^5\text{-}C_5Me_5Cr(CO)_2PMe_2Ph\}$ with CO, which exhibits a relatively high enthalpy of activation and a near zero entropy of activation. The latter parameter is suggestive of a possibile shift toward an interchange mechanism,[14a] the associative pathway possibly becoming increasingly less favorable relative to dissociative activation because of severe steric interactions of the leaving phosphine with the $\eta^5\text{-}C_5Me_5$ ligand in the complex. Performing the studies at high pressure to yield volume of activation parameters may provide further mechanistic information on these systems.[14b]

In the course of this investigation, we have also obtained information concerning equilibrium constants, K_{sub}, at 302 K for some of the reactions represented by eq 2. For substitution reactions of $\{\eta^5\text{-}C_5H_5Cr(CO)_3\}$ with CDPP and $PMePh_2$, K_{sub} decreases in the order $PMePh_2$ (260 ± 85) > CDPP (0.47 ± 0.04), while for reactions of $\{\eta^5\text{-}C_5Me_5Cr(CO)_3\}$ with $PMePh_2$ and PMe_2Ph, K_{sub} decreases in the order PMe_2Ph (0.41 ± 0.06) > $PMePh_2$ (0.075 ± 0.036). Thus there seems to be a clear correlation between position of equilibrium and degree of steric crowding in the products, although we have assessed the relative contributions of the enthalpy and entropy contributions only in the case of the reaction of $\{\eta^5\text{-}C_5H_5Cr(CO)_3\}$ with CDPP ($\Delta H = 8.2 \pm 5.7$ kJ mol^{-1}, $\Delta S = 20.4 \pm 18$ J mol^{-1} K^{-1}).

Disproportionation Reactions. Disproportionation reactions of the type shown in eq 3 have been reported previously for reactions of $[\eta^5\text{-}C_5H_5Cr(CO)_3]_2$ with several chelating diphosphines[5f] and a single monodentate phosphine, PMe_3.[6h] Although the emphasis in this work was on the substitution reactions, our preliminary explorations of these did reveal that substitution by PMe_2Ph could be accompanied by disproportionation to give the monosubstituted complex $[\eta^5\text{-}C_5H_5Cr(CO)_3(PMe_2Ph)][\eta^5\text{-}C_5H_5Cr(CO)_3]$, identified by its IR and ^1H NMR spectrum.

---

(14) (a) Langford, C. H.; Gray, H. B. *Ligand Substitution Processes*; Benjamin: New York, 1965. (b) Wieland, S.; van Eldik, R. *Organometallics* 1991, *10*, 3110.

Subsequent further substitution of the cation to give $[\eta^5\text{-}C_5H_5Cr(CO)_2(PMe_2Ph)_2][\eta^5\text{-}C_5H_5Cr(CO)_3]$ also occurs readily; this new compound was isolated and characterized spectroscopically and by elemental analyses, while the related complex, $[\eta^5\text{-}C_5H_5Cr(CO)_2(PMe_3)_2][\eta^5\text{-}C_5H_5Cr(CO)_3]$, was identified spectroscopically by comparison with data in the literature.[6h] Species of the type $[\eta^5\text{-}C_5H_5Cr(CO)_2L_2][\eta^5\text{-}C_5H_5Cr(CO)_3]$ are normally observed when disproportionation reactions occur at ambient temperature.

Although we have not carried out a kinetic study of the disproportionation reactions, the fact that they have been observed only in reactions of $\{\eta^5\text{-}C_5H_5Cr(CO)_3\}$ with the smaller phosphines and are favored by higher concentrations of reactants suggests that a mechanism of the type found for disproportionation reactions of $V(CO)_6$[15] may apply. This would involve bimolecular formation of monosubstituted radical, as in eq 2, followed by interaction of this radical with a second molecule of $\{\eta^5\text{-}C_5H_5Cr(CO)_3\}$ via a bridging isocarbonyl interaction, i.e., $\{\eta^5\text{-}C_5H_5L(OC)CrCO{:}\!\rightarrow Cr(CO)_3(\eta^5\text{-}C_5H_5)\}$.

Electron transfer would follow, a process that would be facilitated when L is a relatively small, basic ligand.

Alternatively, disproportionation may occur via the 19-electron intermediate $\{\eta^5\text{-}C_5H_5Cr(CO)_3L\}$, as in eqs 5 and 6.[4c]

$$\{\eta^5\text{-}C_5H_5Cr(CO)_3\} + L \rightarrow \{\eta^5\text{-}C_5H_5Cr(CO)_3L\} \quad (5)$$

$$\{\eta^5\text{-}C_5H_5Cr(CO)_3L\} + \{\eta^5\text{-}C_5H_5Cr(CO)_3\} \rightarrow [\eta^5\text{-}C_5H_5Cr(CO)_3L]^+ + [\eta^5\text{-}C_5H_5Cr(CO)_3]^- \quad (6)$$

The latter process is probably favored, since the monosubstituted cation $[\eta^5\text{-}C_5H_5Cr(CO)_3(PMePh_2)]^+$ was observed in a low-temperature NMR study.

X-ray Crystal Structure of $\eta^5\text{-}C_5H_5Cr(CO)_2(CDPP)H$. The structure of this compound is illustrated in Figure 1, while bond distances and angles are given in Table II. Although the position of the hydride ligand could not be determined, occupation of the apparent vacant site by the hydride would result in a cisoid four-legged piano stool type structure. The chromium–carbonyl and chromium–phosphorus bond lengths are similar to those in the 18-electron complexes *cis*- and *trans*-$[\eta^5\text{-}C_5Me_5Cr(CO)_2\{P(OMe)_3\}_2{}^+]$[16] and those in the 17-electron complexes $\{\eta^5\text{-}C_5H_5Cr(CO)_2(PPh_3)\}$[5a] and $\{\eta^5\text{-}C_5Me_5Cr(CO)_2(PMe_3)\}$.[5i] The OC–Cr–CO bond angle is 83.3 (2)° and the OC–Cr–P4 bond angles 86.7 (2)° (cisoid) and 106.2 (2)° (transoid); while ligand–metal–ligand bond angles are known to vary significantly in similar compounds of molybdenum,[17] few such structural data seem available for compounds of chromium.

Acknowledgment. Financial support from the Natural Sciences and Engineering Research Council of Canada (operating grants to D.H.M. and M.C.B.) made this research possible. We also thank J. A. Stone, J. R. Norton, and A. J. Poë for helpful discussions and Dr. G. Silverman, of M & T Chemicals, for gifts of CDPP and DCPP.

Supplementary Material Available: Tables of fractional coordinates and isotropic displacement parameters for all atoms and temperature factor expressions and a derivation of the rate law used (9 pages). Ordering information is given on any current masthead page.

OM9107909

---

[15] Richmond, T. G.; Shi, Q.-Z.; Trogler, W. C.; Basolo, F. *J. Am. Chem. Soc.* **1984**, *106*, 76.

[16] Salsini, L.; Pasquali, M.; Zandomeneghi, M.; Festa, C.; Leoni, P.; Braga, D.; Sabatino, P. *J. Chem. Soc., Dalton Trans.* **1990**, 2007.

[17] See footnote in ref 5f.

Mechanistic Study of Hydrogen Activation by Cationic Dinuclear (μ-Sulfido)molybdenum Complexes

Linda L. Lopez, P. Bernatis, J. Birnbaum, R. C. Haltiwanger, and M. Rakowski DuBois*

Department of Chemistry and Biochemistry, University of Colorado, Boulder, Colorado 80309

Received March 4, 1992

The cationic derivatives $[(MeCpMo)_2(S_2CH_2)(\mu\text{-}S)(\mu\text{-}SR)]X$ (R = C_4H_3S, CH_2CO_2Me; X = Br, SO_3CF_3; MeCp = $C_5H_4CH_3$) have been synthesized and characterized spectroscopically. A single crystal of $[(MeCpMo)_2(S_2CH_2)(\mu\text{-}S)(\mu\text{-}SC_4H_3S)]Br$ has been studied by X-ray diffraction. The complex crystallized in space group $P2_1/n$ with $a = 7.030$ (3) Å, $b = 19.777$ (8) Å, $c = 15.106$ (6) Å, $\beta = 90.84$ (3)°, and $Z = 4$. The structure showed that the μ-thiophenethiolate ligand was oriented away from the adjacent sulfido ligand. The reactions of the cationic derivatives with hydrogen have been studied. The bromide salts reacted with hydrogen to form RH, $(MeCpMoS)_2S_2CH_2$, and 1 equiv of HBr. In the presence of a nitrogen base, the reactions of the cations with hydrogen proceeded to form the neutral complexes $(MeCpMo)_2(S_2CH_2)(\mu\text{-}SR)(\mu\text{-}SH)$ and 1 equiv of protonated base. The kinetics of the latter hydrogen activation reaction have been studied over a range of temperatures, hydrogen pressures, and base concentrations. The kinetic data are consistent with a rate law which is first order in cation and first order in hydrogen. For the cation where R = CH_2CO_2Me, the deuterium isotope effect, k_H/k_D, was found to be 2.5 at 50 °C and the following activation parameters were determined: $\Delta H^{\ddagger} = 84$ kJ/mol and $\Delta S^{\ddagger} = -9$ J/(mol K). The data seem most consistent with a heterolytic mechanism for the activation of hydrogen. Several possible mechanisms for hydrogen addition to the cation are discussed. Attempts to model the initial hydrogen addition product have been made by reacting the related neutral complexes $(CpMo)_2(S_2CH_2)(\mu\text{-}SMe)(\mu\text{-}SR)$ with 1 equiv of strong anhydrous protic acid. The reactions with acid involved either protonolysis of thiolate ligands or oxidation of the dimer, depending on the nature of thiolate substituents. However, no protonated intermediates were detected.

We have reported that some cationic molybdenum sulfide complexes of the general formula $[(CpMo)_2(S_2CH_2)(\mu\text{-}S)(\mu\text{-}SR)]^+$ react with molecular hydrogen to form the final products shown in eq 1. Reaction 1 ulti-

0276-7333/92/2311-2424$03.00/0